

A Radiatively Light Stop Saves the Best Global Fit for Higgs Boson Mass and Decays

Zhaofeng Kang,^{1,2} Tianjun Li,^{1,3} Jinmian Li,¹ and Yandong Liu¹

¹State Key Laboratory of Theoretical Physics and Kavli Institute for Theoretical Physics China (KITPC),
Institute of Theoretical Physics, Chinese Academy of Sciences, Beijing 100190, P. R. China

²Center for High-Energy Physics, Peking University, Beijing, 100871, P. R. China

³George P. and Cynthia W. Mitchell Institute for Fundamental Physics and Astronomy,
Texas A&M University, College Station, TX 77843, USA

(Dated: September 1, 2018)

The LHC discovered the Standard Model (SM) like Higgs boson with mass around 125 GeV. However, there exist hints of deviations from Higgs decays. Including the Tevatron data, the deviations can be explained by the extremely mixed stop sector in the sense of best global fit (BGF). We analyze the relations among the competing reduced coupling hGG , Higgs boson mass, and LHC stop mass $m_{\tilde{t}_1}$ lower bound at the tree- and one-loop level. In particular, we point out that we use the light stop running mass in the Higgs boson mass calculation while the light stop pole mass in the Higgs decays. So the gluino radiative correction on the light stop mass plays the crucial role. Its large negative correction saves the GBF in the Minimal Supersymmetric SM (MSSM) and the next to the MSSM (NMSSM) constrained by the perturbativity. Moreover, a light stop is predicted: in the MSSM if we set the gluino mass $M_3 \lesssim 4$ TeV, we have $m_{\tilde{t}_1} < m_t$; while in the NMSSM, imposing the least tuning condition we get $m_{\tilde{t}_1} \simeq 130$ GeV for $M_3 \simeq 1.5$ TeV.

Introduction: The LHC has not found any direct signature of supersymmetry (SUSY) so far. But at the 5σ level the discovery of the Standard Model (SM)-like Higgs boson with mass $m_h \simeq 125$ GeV [1, 2], indirectly supports SUSY from several aspects. In the first, if this spin-0 particle is confirmed as a fundamental particle, we must explain the corresponding quadratic divergency problem, and SUSY is the most elegant solution. Next, one may wonder why the Higgs boson is so light, *i.e.*, why is it not 150 GeV or even heavier? But this is not a puzzle in the SUSY models, which actually are suffering from the opposite puzzle: why is the Higgs boson so heavy?

Last but never the least, the discovered Higgs boson is not exactly SM-like and shows some notable deviations which may imply new physics. Both the gluon fusion (GF) and vector boson fusion (VBF) production modes show significant di-photon excess. For the $pp \rightarrow h \rightarrow V^*V$ channel there exists a mild deficit in the CMS experiment [2] but small excess in the ATLAS experiment [1]. Including the Tevatron data, the best global fit (BGF) gives [3]

$$c_g^2 = \frac{\Gamma(h \rightarrow gg)}{\Gamma^{\text{SM}}(h \rightarrow gg)} \approx 0.7, \quad c_\gamma^2 = \frac{\Gamma(h \rightarrow \gamma\gamma)}{\Gamma^{\text{SM}}(h \rightarrow \gamma)} \approx 2.1, \quad (1)$$

with all the other couplings fixed. The reduced couplings $c_{g,\gamma}$ are sensitive to colored and/or charged particles beyond the SM, and thus indicating new physics.

In SUSY models, stau can increase c_γ but does not affect c_g [6] while the stops, which carry the $SU(3)_C$ and $U(1)_{EM}$ quantum numbers simultaneously, may alter the reduced couplings towards Eq. (1). Practically, if the stop-loop interferes destructively with the top-loop contributing to $h \rightarrow gg$ while constructively with the W -loop contributing to $h \rightarrow \gamma\gamma$, then the stops can improve the global fit by an amount $\Delta\chi^2 \sim 10$ (compared to the SM fit). However, the above BGF in Eq. (1) can not be realized generically in the SUSY models due to the relatively large SM-like Higgs boson mass. In this

letter, we investigate the possibility of accommodating such BGF in the conventional minimal supersymmetric SM (MSSM) and the next-to-the MSSM (NMSSM) [4]. We find that the BGF can be obtained if the gluino radiative correction to the light stop pole mass is negative and large.

c_g competing with m_h and $m_{\tilde{t}_1}$: The stop sector is the focus of SUSY phenomenology right now due to various reasons. Firstly, the stop corrections [7] lift m_h above the LEP bound and even to 125 GeV indicated by the LHC. At the one-loop level, the corrections can be approximated as

$$\Delta_t \simeq \frac{3m_t^4}{4\pi^2 v^2} \left(\log \left(\frac{m_t^2}{m_{\tilde{t}}^2} \right) + \eta_t^2 \left(1 - \frac{\eta_t^2}{12} \right) \right), \quad (2)$$

with $v = 174.6$ GeV, $\eta_t = X_t/m_{\tilde{t}}$ with $X_t \equiv A_t - \mu \cot \beta$ the stop mixing parameter, and $m_{\tilde{t}} = \sqrt{m_{\tilde{t}_1} m_{\tilde{t}_2}}$ the geometric mean of two stop masses. Here, A_t is the top quark trilinear soft term and μ is the Higgs bilinear mass term in superpotential. When $\eta_t \ll 1$, the mixing term is ignorable and the leading logarithm dominates the corrections. While in the maximal mixing scenario with $\eta_t \approx \sqrt{6}$ [8], the mixing term effect maximizes. However, as $\eta_t > 2\sqrt{3}$ this effect begins to act reversely. We will find that it is the typical case to approach the BGF.

Next, the stop sector can change the reduced couplings of hGG and $h\gamma\gamma$ simultaneously. In terms of the BGF in Eq. (1), the stop-loop should destructively interfere with the top-loop and thus modify the total reduced hGG coupling to be [9]

$$c_g \approx 1 + \frac{1}{4} \left(\frac{m_t^2}{m_{\tilde{t}_1}^2} - \eta_t^2 \frac{m_t^2}{m_{\tilde{t}}^2} \right) \sim -0.84, \quad (3)$$

where the heavier stop contribution is ignored. Accord-

ingly, the reduced $h\gamma\gamma$ coupling is modified to be [9]

$$c_\gamma \approx 1.28 - 0.28c_g, \quad (4)$$

which is valid for $m_h \simeq 125$ GeV and $c_V \simeq 1$.

Finally, the stops carry colour charges and have a close relation with the pattern of electroweak symmetry breaking. Thus, they are among the main search particles at the LHC. Presently, the lighter stop is bounded by $m_{\tilde{t}_1} \gtrsim 130$ GeV (details is postponed). Then we get $m_{\tilde{t}_L} \gtrsim 600$ GeV from the approximation which is valid for highly mixed stops:

$$m_{\tilde{t}_L} \approx (2C_G)^{1/2} m_{\tilde{t}_1}, \quad |X_t| \approx (2C_G)^{1/2} \frac{m_{\tilde{t}_1}}{m_t} m_{\tilde{t}_L}, \quad (5)$$

with $C_G \approx 4(1 - c_g) + m_t^2/m_{\tilde{t}_1}^2$. We have taken the simplifying assumption $m_{\tilde{t}_R} = m_{\tilde{t}_L}$, but it can be abandoned.

Synthesizing these aspects, we obtain the competing relations among c_g and m_h , $m_{\tilde{t}_1}$, which make it difficult to realize the BGF in the (N)MSSM. (A) At least in the MSSM, to get $m_h \simeq 125$ GeV a large $m_{\tilde{t}_1}$ and properly mixed stop sector are necessary. It means that generically the mixing term in Eq. (3) is ignorable, while the lighter stop enhances c_g instead of the other way around. (B) The NMSSM, in spite of its advantage in lifting m_h which weakens the relation with the stop sector, is also impossible. This is blamed to the lower bound on $m_{\tilde{t}_L}$, which leads to a big suppressing $m_t^2/m_{\tilde{t}_1}^2 \ll 1$ in c_g . Consequently, if the mixing term can still make $c_g \sim -0.8$, we likely need $\eta_t > 12$ to compensate for that. In turn, such a large mixing term, which grows quartically in Δ_t , will decrease m_h . However, this behavior is only an approximation, and it underestimates Δ_h in the large mixing region. In the numerical plot we will adopt the complete expression.

A radiatively light stop mass as a savior: The previous robust relations from the two-parameters stop system can be relaxed, if we take into account the sizeable one-loop radiative correction to the lighter stop (the much smaller correction to the heavier stop is neglected here). Such correction is crucial, since the stop mass used to calculate Δ_t is the running $\overline{\text{DR}}$ mass, while the stop mass in Eq. (3), used to calculate c_g , is the pole mass. They are related by the equation

$$m_{\tilde{t}_1}^2 = m_{\tilde{t}_1}^2(Q) - \text{Re}(\Pi(p^2, Q))|_{p^2=m_{\tilde{t}_1}^2}, \quad (6)$$

where the running mass $m_{\tilde{t}_1}(Q)$ is defined at the renormalization scale $Q = m_{\tilde{t}_L}$. $\Pi(p^2, Q)$ is the self-energy, dominated by the QCD and top-Yukawa radiative corrections from the gluon, gluino, stop and chargino loop, etc. When the positive self-energy is sufficiently large, the pole mass can be much lighter than the running mass.

The gluino mass plays the primary role to reduce the running mass. There exists some uncertainties from the Yukawa and two-loop corrections. In the analytical analysis we will not go through the details of this discussion, but instead introduce an extra parameter ω_t , the ratio of

pole mass and running mass, to account for those. Illustratively, at the order $\mathcal{O}(\alpha_s)$, ω_t is roughly given by [10]

$$\omega_t \approx 1 + \frac{2}{3} \frac{\alpha_s}{\pi} \left[\frac{2M_3^2}{m_{\tilde{t}_1}^2(Q)} \left(1 - \ln \frac{M_3^2}{Q^2} \right) - \frac{m_{\tilde{t}_2}^2(Q)}{2m_{\tilde{t}_1}^2} \left(1 - \ln \frac{m_{\tilde{t}_2}^2(Q)}{Q^2} \right) \right]_{Q=m_{\tilde{t}_L}} \quad (7)$$

The approximation is valid for $M_3, m_{\tilde{t}_2}(Q) \gg m_{\tilde{t}_1}(Q) \sim m_t$. Note that we have $m_{\tilde{t}_2} > Q$. Given a heavy gluino (required by the LHC bound), the running mass can readily be reduced by a factor 2 or 3. As a consequence, one can work in the maximal mixing scenario $\eta_t^2(m_{\tilde{t}_L}) \simeq 6$, while $\eta_t^2(\text{pole})$ is several times larger than $\eta_t^2(m_{\tilde{t}_L})$. In this way, the radiatively reduced stop mass offers a solution to reconcile the serious tension between m_h and c_g .

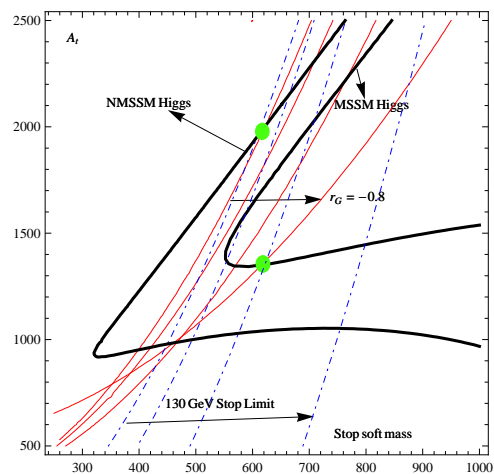


FIG. 1: Schematic plots of $m_h = 125$ GeV, $c_g = -0.8$ (red thin solid lines) and $m_{\tilde{t}_1} = 130$ GeV (dashed lines) on the $m_{\tilde{t}_L} - X_t$ plane. For comparison, we choose $\omega_t = 0.5, 0.4, 0.3, 0.2$ for c_g and $m_{\tilde{t}_1}$, respectively from the left to right. In plotting m_h we have fixed $\tan\beta = 25$ in the MSSM and $\tan\beta = 2$, $\lambda = 0.6$ in the NMSSM. The running top mass is taken to be 155 GeV.

The schematic analysis in Fig. 1 manifests the point. In the MSSM, as ω_t decreases the $c_g = -0.8$ curves, which are denoted by the red solid lines, move towards the left and meet with the $m_h = 125$ GeV curve at a large $m_{\tilde{t}_L}$. As for the NMSSM, such meeting still needs $\omega_t \lesssim 0.6$ (we will turn back to this point later). In this case, the lower bound on the stop pole mass $m_{\tilde{t}_1} = 130$ GeV means that the running mass is above 220 GeV. In turn, we require a rather heavy gluino mass to account for the big gap. Additionally, from Fig. 1 one can see that for a given ω_t , the $c_g = -0.8$ curve intersects with the $m_{\tilde{t}_1} = 130$ GeV curve at large $m_{\tilde{t}_L}$ (understood similarly to Eq. (5)). And its value increases as ω_t decreases.

$\omega_t \lesssim 0.6$ is owing to the NMSSM perturbativity up to M_{GUT} . It renders $\lambda \lesssim 0.7$ and imposes the tree-level

bound $m_h \lesssim \lambda v \sin \beta \simeq 110 \text{ GeV}$. Then a moderate stop correction and/or pushing effect is still indispensable. In turn, in light of the relations between competing $m_{\tilde{t}_1}$, m_h and c_g , the NMSSM with $w_t \sim 1$ fails. But in ASUSY [11] with $\lambda \sim 2$, or other non-decoupling F/D -term models [12], tree-level m_h can be sufficiently heavy such that large $\eta_t (> 12)$ is endured.

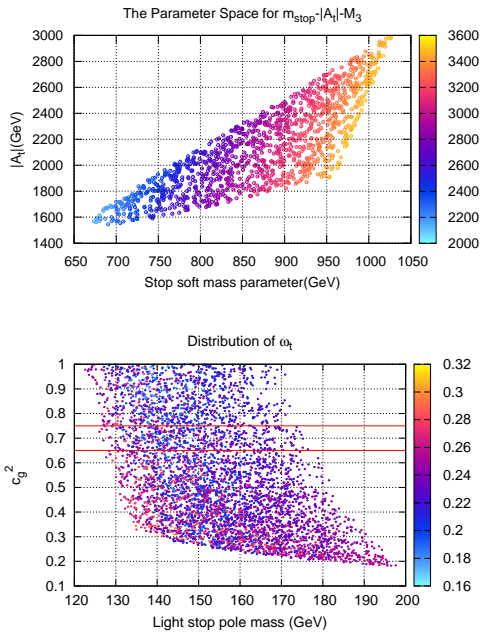


FIG. 2: Top figure: The plot of the parameter space for $m_{\tilde{t}_L}-|A_t|-M_3$, where we have required $0.7 < c_g^2 < 0.8$ and $123 \text{ GeV} < m_h < 127 \text{ GeV}$; Bottom figure: The plot of distribution of w_t .

Numerical search in the (N)MSSM: For a more precisely quantitative study, we turn to the NMSSM-Tools 3.2.0 [13]. Firstly we get the MSSM limit from the NMSSM, e.g., setting it to the decoupling limit: $\lambda = \kappa = 0.01$, $\tan \beta = 15$, $\mu = 500 \text{ GeV}$, $A_\kappa = 800 \text{ GeV}$, $M_A = 1.5 \text{ TeV}$. One may vary them freely, but it will not bring much difference to the configuration of the three-parameter-space $m_{\tilde{t}_L}-|A_t|-M_3$, projected on the $m_{\tilde{t}_L}-|A_t|$ plane. From Fig. 2, it is seen that the right edge of the triangle can extend when we increase M_3 , etc. Accordingly, the right edge of the ω_t distribution slowly moves towards the right, where w_t becomes smaller. In summary, a multi-TeV gluino, $|A_t|$ and quite small ω_t are the main features of the parameter space in the MSSM.

Now we turn our attention to the limit which manifests the NMSSM specific effects enhancing m_h [14, 15]. It is characterized by $\lambda \sim 1$, $\tan \beta \sim 1$ and/or a small μ . Especially, a small μ , which is consistent with naturalness, leads to not only the Higgs doublet-singlet (HS) mixing pushing upward m_h [14] but also the di-photon excess by suppressing $\text{Br}(h \rightarrow b\bar{b})$ [14, 16]. But in view of the BGF, the stop-loop instead of the mixing effect should

account for the excess. Therefore, we require a small HS mixing angle such that hff and hVV are not modified much, as forces us to accept some degree of tuning, from either a relatively large μ or a mild cancellation in the Higgs mass matrix.

We restrict the discussion to a smaller μ and explore how natural the NMSSM can be after requiring the BGF. Roughly speaking, this amounts to find the gluino lower bound [9, 14], which has been shown to be large. $|A_t|$ also should be sufficiently small [9, 14, 17]. We give a benchmark point here. The inputs at the SUSY scale are $M_1 = 110 \text{ GeV}$, $M_2 = 740 \text{ GeV}$, $M_3 = 1500 \text{ GeV}$, $A_t = -1530 \text{ GeV}$, and $m_{\tilde{t}_L} = 588 \text{ GeV}$. Also, $\tan \beta$, μ and the NMSSM specified parameters are $\tan \beta = 2.17$, $\lambda = 0.666$, $\kappa = 0.253$, $A_\lambda = 510 \text{ GeV}$, $A_\kappa = -248 \text{ GeV}$, and $\mu = 291 \text{ GeV}$. The resulting particle spectra contains the SM-like Higgs, light stop and lightest neutralino with the dominant bino component. Their pole masses are given by $m_h = 124.8 \text{ GeV}$, $M_{\chi_1^0} = 100.0 \text{ GeV}$, and $m_{\tilde{t}_1} = 130.3 \text{ GeV}$. In particular, $c_g = -0.84$ is generated.

We would like to make some comments. (A) The stop-chargino loop generates flavor transition $b \rightarrow s\gamma$. However, its rate is safely small if we take $\tan \beta \lesssim 20$ and μ a few hundred GeV [18]. (B) Due to the large A_t -term, the split stop-sbottom may render $\Delta\rho$ orders larger than the experimentally allowed bound $\lesssim 10^{-3}$. Small $m_{\tilde{t}_L}$ is favored to lower the size of $\Delta\rho$, and some cancellation from $m_{\tilde{b}_R}$ is needed. (C) We can relax the lower bound on $m_{\tilde{t}_1}$ slightly, e.g., to 125 GeV , by means of introducing R -parity violation operators $U^c D^c D^c$. It makes the very light stop missed at the LHC due to the absence of missing transverse energy. In this case, we do not need the heavy gluino and the BGF can be naturally realized in the NMSSM.

A light stop escapes from the LHC: In both models, if $M_3 < 4 \text{ TeV}$, we predict $m_{\tilde{t}_1} \lesssim m_t$, see Fig. 2. As long as we impose the minimal fine-tuning condition, it is found that the NMSSM allows $M_3 \lesssim 1.5 \text{ TeV}$ and gives $m_{\tilde{t}_1} \simeq 130 \text{ GeV}$ which will be checked safe.

The LHC search for the stop is sensitive to its decay topology and the particle spectrum. As a case in point, we consider the benchmark point in the NMSSM. It contains the relevant particles, *i.e.*, the light stop with mass 130 GeV and the 100 GeV bino-like neutralino LSP χ_1^0 . Due to the kinematics under consideration, \tilde{t}_1 dominantly (nearly 100%) decays to c and χ_1^0 via the loop-induced process. The process at the LHC is

$$gg \rightarrow \tilde{t}_1 \tilde{t}_1^* \rightarrow c + \bar{c} + 2\chi_1^0. \quad (8)$$

In this case, the monojet and jets+ E_T^{miss} signatures give the strongest bounds [19]. Actually, the monojet bound is effective only when $0 < m_{\tilde{t}_1} - m_{\chi_1^0} < 0.2m_{\chi_1^0}$. Otherwise, a putative case in this work, it is ineffective and need the inspection to jets+ E_T^{miss} , discussed in the following.

At first, we use MadGraph5 v1.4.7 [20] to generate the stop pair, accompanied by (≤ 3) additional initial state radiative (ISR) jets. In calculating this cross section, we

take the modified MLM matching with $xqcut = 30$ GeV and shower-kt scheme with $QCUT=50$ GeV. Then after matching the LO production cross sections of $\tilde{t}_1\tilde{t}_1^* + nj$ at the 7 TeV LHC, are displayed in the following:

Channel	$\tilde{t}\tilde{t}$	$\tilde{t}\tilde{t} + j$	$\tilde{t}\tilde{t} + jj$	$\tilde{t}\tilde{t} + (\geq 3j)$
Cross section (pb)	42.08	15.73	3.84	0.87

Moreover, the k-factor calculated by the Prospino2 [21] is about 1.5 for $m_{\tilde{t}_1} \sim 130$ GeV. After these, we use Pythia to do the particle decay, parton showering and hadronization [22]. PGS is chosen to simulate the detector effect. Finally, employing the cuts adopted in Ref [23], we find that only the events with two or more ISR jets survive. The most sensitive signal regions and the corresponding event numbers (normalized to 4.7/fb) are given by:

Signal Region	SRC-med	SRC-loo	SRE-med	SRE-loo
Number of Event	2.03(18)	15.10(58)	1.02(12)	4.07(84)

where the numbers in the brackets are the observed upper limits on the event numbers beyond the SM. Clearly, the present ATLAS jets+ E_T^{miss} search can not exclude our light stop scenario. We are awaiting the ongoing LHC to probe such scenarios.

Conclusions and discussions: Stops are potential to accommodate the BGF. At first glances, due to the relations among the competing c_g , $m_{\tilde{t}_1}$, and m_h , there is

merely a sporting chance to realize the BGF in the MSSM and NMSSM. Fortunately, the gluino radiative correction on the light stop mass can make its pole mass much lighter than the running mass, and then the BGF can be realized. If we reasonably let M_3 and $|A_t|$ below 4 TeV, a light stop typically below the top mass is predicted. In particular, in the NMSSM we explore the less fine-tuned region to the most extent, and find that the model allows $M_3 \simeq 1.5$ TeV as well as $m_{\tilde{t}_1} \approx 130$ GeV. Such light stop is not excluded by the ATLAS latest data since the decay $\tilde{t}_1 \rightarrow c + \chi_1^0$ with χ_1^0 about 100 GeV. We encourage the LHC experiments to tailor a search for the light stop inspired by the Higgs BGF. Moreover, besides the light stop, the lightest neutralino, which may be an successful dark matter candidate, also deserves further attention. In our scenario, its mass falls into the region $m_{\tilde{t}_1} > M_{\chi_1^0} > 0.83m_{\tilde{t}_1}$, *i.e.*, between 100 GeV and the m_t . We leave it for a future study. Finally, after the completion of this work we are aware of [24], which gives a stringent constraint on the BGF inspired stop sector from the vacuum stabilities. But their constraint is based on a rather simplified analysis and only valid at the tree-level.

Acknowledgements: This work was supported by the National Natural Science Foundation of China under grant Nos. 10821504, 11075194, and 11135003, and by the DOE grant DE-FG03-95-Er-40917.

-
- [1] G. Aad *et al.* [ATLAS Collaboration], arXiv:1207.7214.
[2] S. Chatrchyan *et al.* [CMS Collaboration], arXiv:1207.7235 [hep-ex].
[3] P. P. Giardino, K. Kannike, M. Raidal and A. Strumia, arXiv:1207.1347; M. R. Buckley and D. Hooper, arXiv:1207.1445; D. Carmi, *et al.*, arXiv:1207.1718.
[4] U. Ellwanger, C. Hugonie and A. M. Teixeira, Phys. Rept. **496**, 1 (2010).
[5] M. A. Ajaib, I. Gogoladze and Q. Shafi, arXiv:1207.7068; J. R. Espinosa, C. Grojean, V. Sanz and M. Trott, arXiv:1207.7355.
[6] M. Carena, S. Gori, N. R. Shah and C. E. M. Wagner, JHEP **1203**, 014 (2012); J. Ke, M. -X. Luo, L. -Y. Shan, K. Wang and L. Wang, arXiv:1207.0990; G. F. Giudice, P. Paradisi and A. Strumia, arXiv:1207.6393.
[7] Y. Okada, *et al.*, Prog. Theor. Phys. **85**, 1 (1991).
[8] J. R. Ellis, G. Ridolfi and F. Zwirner, Phys. Lett. B **262**, 477 (1991); Z. Kang, *et al.*, arXiv:1203.2336; F. Brummer, S. Kraml and S. Kulkarni, arXiv:1204.5977.
[9] K. Blum, R. T. D'Agnolo and J. Fan, arXiv:1206.5303.
[10] D. M. Pierce, J. A. Bagger, K. T. Matchev and R. -j. Zhang, Nucl. Phys. B **491**, 3 (1997).
[11] R. Barbieri, L. J. Hall, Y. Nomura and V. S. Rychkov, Phys. Rev. D **75**, 035007 (2007); L. J. Hall, D. Pinner and J. T. Ruderman, JHEP **1204**, 131 (2012); E. Hardy, J. March-Russell, and J. Unwin, arXiv:1207.1435.
[12] T. Basak and S. Mohanty, arXiv:1204.6592; M. Hirsch, *et al.*, arXiv:1206.3516; C. Cheung and H. L. Roberts, arXiv:1207.0234; H. An, T. Liu and L. -T. Wang, arXiv:1207.2473.
[13] U. Ellwanger and C. Hugonie, Comput. Phys. Commun. **175** (2006) 290; U. Ellwanger, J. F. Gunion, and C. Hugonie, JHEP **02** (2005) 066.
[14] Z. Kang, J. Li and T. Li, arXiv:1201.5305.
[15] U. Ellwanger, JHEP **1203**, 044 (2012); J. F. Gunion, *et al.*, Phys. Lett. B **710**, 454 (2012); D. A. Vasquez, *et al.*, arXiv:1203.3446; K. S. Jeong, *et al.*, arXiv:1205.2486; R. Benbrik, *et al.*, arXiv:1207.1096; B. Kyae and J. -C. Park, arXiv:1207.3126; J. Cao, *et al.*, arXiv:1207.3698; T. Cheng, *et al.*, arXiv:1207.6392.
[16] U. Ellwanger, Phys. Lett. B **698** (2011); J. Cao, *et al.*, Phys. Lett. B **703**, 462 (2011).
[17] C. Wymant, arXiv:1208.1737.
[18] S. Bertolini, F. Borzumati, A. Masiero and G. Ridolfi, Nucl. Phys. B **353**, 591 (1991).
[19] B. He, T. Li and Q. Shafi, JHEP **1205**, 148 (2012); X. -J. Bi, Q. -S. Yan and P. -F. Yin, Phys. Rev. D **85**, 035005 (2012); M. Drees, M. Hanussek and J. S. Kim, arXiv:1201.5714.
[20] J. Alwall, M. Herquet, F. Maltoni, O. Mattelaer and T. Stelzer, JHEP **1106**, 128 (2011).
[21] W. Beenakker, R. Hopker and M. Spira, hep-ph/9611232.
[22] T. Sjostrand, S. Mrenna and P. Z. Skands, JHEP **0605**, 026 (2006).
[23] ATLAS Collaboration, ATLAS-CONF-2012-033
[24] M. Reece, arXiv:1208.1765.